Published in final edited form as:
Nanomedicine. 2014 October ; 10(7): 1385–1388. doi:10.1016/j.nano.2014.05.001.

MR Cholangiography Demonstrates Unsuspected Rapid Biliary Clearance of Nanoparticles in Rodents: Implications for Clinical Translation

Jeff W.M. Bulte, PhD[1,*], **Anne H. Schmieder, MS**[2], **Jochen Keupp, PhD**[3], **Shelton D. Caruthers, PhD**[2,3], **Samuel A. Wickline, MD**[2], and **Gregory M. Lanza, MD PhD**[2]

[1]Russell H. Morgan Department of Radiology and Radiological Science, Division of MR Research and Cellular Imaging Section, Institute for Cell Engineering, the Johns Hopkins University School of Medicine, Baltimore, MD 21205

[2]Department of Medicine, Division of Cardiology, Washington University Medical School, St. Louis, MO 63108

[3]Philips Healthcare, Cleveland, OH 44143

[4]Philips Research, Hamburg, Germany

Abstract

Due to their small size, lower cost, short reproduction cycle, and genetic manipulation, rodents have been widely used to test the safety and efficacy for pharmaceutical development in human disease. In this report, MRI cholangiography demonstrated an unexpected rapid (<5 min) biliary elimination of gadolinium-perfluorocarbon nanoparticles (approximately 250 nm diameter) into the common bile duct and small intestine of rats, which is notably different from nanoparticle clearance patterns in larger animals and humans. Unawareness of this dissimilarity in nanoparticle clearance mechanisms between small animals and humans may lead to fundamental errors in predicting nanoparticle efficacy, pharmacokinetics, biodistribution, bioelimination, and toxicity.

Keywords

Nanoparticle; hepatobiliary clearance; rat; MRI; MR contrast agent; cholangiography

Correspondence: Jeff W.M. Bulte, Ph.D., The Johns Hopkins University School of Medicine, Russell H. Morgan Department of Radiology and Radiological Science, Division of MR Research, 217 Traylor Bldg, 720 Rutland Ave, Baltimore, MD 21205, Phone 443-287-0996, Fax 443-287-7945, jwmbulte@mri.jhu.edu.

Conflicts of Interest: GML and SAW are scientific co-founders of Kereos, Inc. St. Louis, MO, which sublicensed related intellectual property from Washington University Medical School. SDC and JK are employees of Philips Healthcare

Prior presentations or earlier publication in abstract form:
These data were partially presented at the 6th Annual Meeting of the International Society of Magnetic Resonance in Medicine, Sydney, Australia, 1998. (Proc. of ISMRM 6th Annual meeting, 209, 1998).

Background

Many years ago (around 1998), our laboratories began to study the use of 250 nm paramagnetic perfluorocarbon nanoparticles (NP) in rats. In these early studies, biliary excretion of these paramagnetic particles was observed a few minutes after intravenous injection, enabling the creation of MR cholangiograms, perhaps the first ever made using nanotechnology[1]. The accumulation of NP in the intestines of rodents was observed innumerable times over subsequent years, but this biodistribution pattern was not appreciated in numerous larger animal models including rabbits[2, 3]. The objective of this communication is to share these observations with the nanocommunity as well as some of the key scientific literature beginning in the late 1950's that previously explored the issue of colloidal clearance in rodents, larger animals, and humans.

Materials and Methods

Preparation and characterization of perfluorocarbon NP

Paramagnetic perfluorocarbon NP were prepared as previously reported[4]. The emulsions were comprised of 40% (v/v) of perfluorooctylbromide (PFOB; Elf Atachem, specific gravity 1.93 g/ml), 2% (w/v) of a surfactant commixture, 1.7% (w/v) glycerin and deionized nanopure water representing the balance. The surfactant mixture consisted of 78 mole% high-purity (>95%) egg yolk phosphatidylcholine, 2 mole% phosphatidylethanolamine, and 20 mole% of the lipophilic gadolinium chelate diethylene-triamine-pentaacetic acid-bis-oleate (Gd-DTPA-BOA; Gateway Chemical Technologies). PFOB, glycerin, and the surfactant commixture were pre-blended with sonication and microfluidized at 14,000 PSI for 4 minutes (Microfluidics, Newton, MA, USA). PFOB particles in example 2 were produced with 20% v/v PFOB and excluded Gd-DTPA-BOA from the surfactant mixture, which was replaced with high purity (>95%) egg yolk phosphatidylcholine on an equimolar basis. Nominal particle sizes were 220±80nm using dynamic light scattering (Malvern Instruments, Malvern, PA) with a polydispersity index <0.2.

MR imaging—All animal studies were conducted in accordance with a protocol approved by the Animal Care and Use Committee of our Institutes

In example 1, 200 g female rats (rnu/rnu) were anesthetized by intraperitoneal (IP) injection of 100 mg/kg ketamine and 10 mg/kg acepromazine. Anesthesia was maintained by administering 25 mg/kg ketamine and 2.5 mg/kg acepromazine IP via a 20-gauge catheter (JELCO, Tampa, FL) every 30 minutes or as needed. Gd-DTPA PFOB NP were injected via tail vein at a dose of 0.05 mmole Gd/kg. MR images were taken before and immediately after injection over a time course of 1 hour. To this end, a Signa 1.5T clinical magnet (General Electric Medical Systems, Milwaukee, WI) was used equipped with a 5-inch circular surface coil and a field of view of 13 cm. A 3D time-of-flight (TOF) spoiled gradient echo (SPGR) sequence was used to obtain coronal images with the following parameters: Echo time (TE)=minimum, flip angle=45 degrees, slice thickness=1.0 mm, matrix=256×192, and number of averages=10. In example 2, PFOB NP were injected via tail vein into a 100 g male Harlan rat at 1.0 ml/kg and allowed to circulate for 2 hours prior to imaging. High-resolution $^{1}H/^{19}F$ MR images were acquired at 3T (Philips Achieva) using

an in-house, custom dual-tuned open birdcage transmit-receive coil[5, 6]. Simultaneous 3D $^{1}H/^{19}F$ imaging was used employing a novel steady state ultrashort echo time (UTE) technique (TE/TR=0.1 ms/1.96 ms) with the frequencies set to the resonance of ^{1}H and the CF_2 groups of the PFOB spectrum (representing 12 of 17 total ^{19}F nuclei)[7]. Using a highly oversampled 3D radial readout scheme, the reconstructed image datasets have a nominal resolution of 1.25 mm[3,8].

Results

In example 1, T1-weighted TOF MR imaging of rats given Gd-DTPA PFOB NP revealed an unexpected rapid biliary excretion. This was appreciated as an MR biliary cholangiogram at 5 minutes following intravenous injection (Figure 1). At baseline, the heart, liver, spleen, and vasculature were not apparent but the gastrointestinal system could be observed secondary to the presence of digesta. One minute post-injection, the blood pool was opacified with NP, clearly revealing the heart, aorta,, and large peripheral vasculature. Highly vascularized organs, such as the liver and spleen, also became visible. Five minutes post-injection, the biliary flow of the injected NP could be clearly appreciated passing from the liver along the common bile duct into the small intestine. The anatomical lack of a gall bladder in the rat was apparent, as these animals do not possess this organ.

In the second example, PFOB NP were injected via tail vein into a rat and simultaneous dual $^{1}H/^{19}F$ MR images were obtained as a 3D stack. Figure 2 presents 4 sequential coronal images of that acquisition. At two hours, a low-level blood pool signal (i.e., colorized green) was appreciated within the cardiac ventricles. As expected, PFOB particles were heavily biodistributed into the liver, producing intense signal in that organ. Consistent with the gadolinium-enhanced images in Figure 1, an abundance of ^{19}F rich PFOB was localized in the small intestines. A tubular ^{19}F-rich reference standard of PFOB NP suspended in agarose is seen on the animal's right. Collectively, these images strongly suggest that entire NP are passing directly and rapidly into the biliary tree and their constituents are flowing into the intestines after i.v. injection.

Discussion

In the present report, rapid biliary excretion of relatively large PFOB NP (~250nm) was observed with T1-weighted 3D TOF and dual $^{1}H/^{19}F$ UTE MR imaging techniques. In man, NP less than 5–6 nm can be bioeliminated through the kidneys and urine, but are otherwise they are retained primarily by the clearance organs belonging to the mononuclear phagocyte system (MPS) until degraded into smaller constitutive elements, which may be metabolized further or eliminated directly via bile, urine, or respiration.[9–12] Although the rapid transit of large, otherwise vascular-constrained particles into the bile and gut was never observed with MRI previously, the scientific appreciation of this phenomena occurred over a century ago.

In 1958, Hampton[13] referenced the 1881 work of Rütimeyer who intravenously administered particles of cinnabar in rodents and reported their distribution into Kupffer cells, hepatic cells, and bile. Hampton further noted that these early results were later corroborated by Müllendorf in 1916 and Weatherford in 1956 using colloidal dyes and India

ink, respectively. Hampton found that colloidal particles (8% HgS in 500 μl or 25% ThO_2, Thorotrast) injected intravenously localized to the liver and spleen with transmission electron microscopy (TEM). Within the liver, they were found in Kupffer cells, hepatocytes, and the biliary tree. Particles phagocytosed by Kupffer cells were retained in those cells indefinitely; whereas particles endocytosed by hepatocytes were transported rapidly into the biliary system. Since systemic protein coating could influence the handling of the particles in the liver, Hampton performed biliary retrograde infusions of Thorotrast colloidal particles. TEM revealed that the particles transited in reverse through hepatocytes into the space of Disse. Some of the Thoratrast was sequestered in Kupffer cells while much passed into the circulatory system. Other evidence of NP excretion into rodent bile and feces include silica particles from 50–200 nm[14], citrate-coated silver particles (~8 nm)[15], and iron oxide core high-density lipoproteins (~10 nm)[16].

In contradistinction to rodents, Juhlin reported in 1960[17] that fluorescent spherical hydrophilic particles of methyl methacrylate injected intravenously in rabbits did not transit effectively into the bile. A 192 mg intravenous injection of particles (20 to 110 nm) produced a minimal biliary concentration of 0.05–0.40 mg/ml during the first minutes after i. v. injection. Fluorescent particles in the range of 60–140 nm were not appreciated in the bile. Further, particles 200–800 nm in diameter were not found in the bile despite a ~10-fold increase in injected dose (1,200 mg).

Rodents are frequently used to characterize the pharmacokinetics, pharmacodynamics, biodistribution, and bioelimination of nanomedicines for basic science and IND regulatory purposes. While these models offers a wealth of research opportunity, the data achieved with nanotechnology must be viewed with an appreciation for the impact of rapid biliary clearance. Rapid excretion of particles along with their therapeutic or imaging payloads substantially lowers the toxicity burden imposed on the animal and can leave a better impression of biosafety than exists. Allometric scaling[18] to project pharmacokinetic data from rodents to man may be inappropriate, since the concept of shape scaling implies that the physiological pathways are conserved. Non-metabolizable particles greater than the renal threshold can pass into the feces of rodents leading to potentially false conclusions of high bioelimination and safety.

In summary, we have presented MRI examples of rapid biliary secretion of relatively large PFOB NP. While the MR cholangiogram using NP may have been the first ever produced in 1998, the recognition that particles can be excreted into the feces via bile in rodents dates back to the 1950s, with the early insights published in the late 19th century. Today, given the rapid expansion of nanomedicine research, it is incumbent upon us to recognize and adjust to the potential translational issues that the use of rodent preclinical models pose on assessments of nanomedicine safety and efficacy studies.

Acknowledgments

The MR images shown in Figure 1 were obtained at the NIH in Vivo NMR Center (Bethesda, MD), with support from Dr. Joseph A. Frank.

Funding: This study was supported by NIH grants CA151838 (JWMB) HL073646 (SAW), HL112518 (GL), HL113392 (GL), CA154737 (GL), CA136398, and NS073457 (GL), and DOD grant CA100623 (GL).

References

1. Bulte JWM, Lanza GM, Fuhrhop R, Kaufman R, Herynek V, Frank JA, Wickline SA. Gd-DTPA perfluorocarbon emulsions as a novel paramagnetic particulate contrast medium: T1 and T2 relaxometry. Proc Int Soc Magn Reson Med. 1998; 6:209.
2. Lijowski M, Caruthers S, Hu G, Zhang H, Scott MJ, Williams T, Erpelding T, Schmieder AH, Kiefer G, Gulyas G, Athey PS, Gaffney PJ, Wickline SA, Lanza GM. High sensitivity: High-resolution SPECT-CT/MR molecular imaging of angiogenesis in the Vx2 model. Invest Radiol. 2008; 43:100–111. [PubMed: 18197062]
3. Winter PM, Morawski AM, Caruthers SD, Fuhrhop RW, Zhang H, Williams TA, Allen JS, Lacy EK, Robertson JD, Lanza GM, Wickline SA. Molecular imaging of angiogenesis in early-stage atherosclerosis with alpha v beta 3-integrin-targeted nanoparticles. Circulation. 2003; 108:2270–2274. [PubMed: 14557370]
4. Flacke S, Fischer S, Scott MJ, Fuhrhop RJ, Allen JS, McLean M, Winter P, Sicard GA, Gaffney PJ, Wickline SA, Lanza GM. Novel MRI contrast agent for molecular imaging of fibrin: Implications for detecting vulnerable plaques. Circulation. 2001; 104:1280–1285. [PubMed: 11551880]
5. Hu L, Hockett FD, Chen J, Zhang L, Caruthers SD, Lanza GM, Wickline SA. A generalized strategy for designing $^{19}F/^{1}H$ dual-frequency MRI coil for small animal imaging at 4.7 tesla. J Magn Reson Imaging. 2011; 34:245–252. [PubMed: 21698714]
6. Hockett F, Wallace K, Schmieder A, Caruthers S, Pham C, Wickline S, Lanza G. Simultaneous dual frequency ^{1}H and ^{19}F open coil imaging of arthritic rabbit knee at 3T. IEEE Trans Med Imaging. 2011; 30:22–27. [PubMed: 20699209]
7. Keupp J, Rahmer J, Grasslin I, Mazurkewitz PC, Schaeffter T, Lanza GM, Wickline SA, Caruthers SD. Simultaneous dual-nuclei imaging for motion corrected detection and quantification of ^{19}F imaging agents. Magn Reson Med. 2011; 66:1116–1122. [PubMed: 21394779]
8. Rahmer J, Keupp J, Caruthers S, Lips O, Williams T, Wickline S, Lanza G. Dual resolution simultaneous $^{19}F/^{1}H$ in vivo imaging of targeted nanoparticles. Proc Int Soc Magn Reson Med. 2009; 17:611.
9. Kaufman, R. Clinical development of perfluorocarbon-based emulsions as red cell substitutes. In: J, S., editor. Emulsions and emulsion stability. New York: Marcel Dekker; 1996. p. 343-367.
10. Mishra S, Heidel JD, Webster P, Davis ME. Imidazole groups on a linear, cyclodextrin-containing polycation produce enhanced gene delivery via multiple processes. J Control Release. 2006; 116:179–191. [PubMed: 16891028]
11. Schluep T, Hwang J, Cheng J, Heidel JD, Bartlett DW, Hollister B, Davis ME. Preclinical efficacy of the camptothecin-polymer conjugate IT-101 in multiple cancer models. Clin Cancer Res. 2006; 12:1606–1614. [PubMed: 16533788]
12. Choi HS, Liu W, Liu F, Nasr K, Misra P, Bawendi MG, Frangioni JV. Design considerations for tumour-targeted nanoparticles. Nat Nanotechnol. 2010; 5:42–47. [PubMed: 19893516]
13. Hampton J. An electron microscope study of the hepatic uptake and excretion of submicroscopic particles injected into the blood stream and the bile duct. Acta Anat. 1958; 32:262–291. [PubMed: 13532240]
14. Cho M, Cho WS, Choi M, Kim SJ, Han BS, Kim SH, Kim HO, Sheen YY, Jeong J. The impact of size on tissue distribution and elimination by single intravenous injection of silica nanoparticles. Toxicology letters. 2009; 189:177–183. [PubMed: 19397964]
15. Park K, Park E, Chun I, Choi K, Lee S, Yoon J, Lee B. Bioavailability and toxicokinetics of citrate-coated silver nanoparticles in rats. Arch Pharm Res. 2011; 34:153–158. [PubMed: 21468927]
16. Skajaa T, Cormode DP, Jarzyna PA, Delshad A, Blachford C, Barazza A, Fisher EA, Gordon RE, Fayad ZA, Mulder WJM. The biological properties of iron oxide core highdensity lipoprotein in experimental atherosclerosis. Biomaterials. 2011; 32:206–213. [PubMed: 20926130]
17. Juhlin L. Excretion of intravenously injected solid particles in bile. Acta Physiol Scand. 1960; 49:224–230. [PubMed: 14408109]
18. Huxley, JS. Problems of relative growth. New York: Dover; 1972.

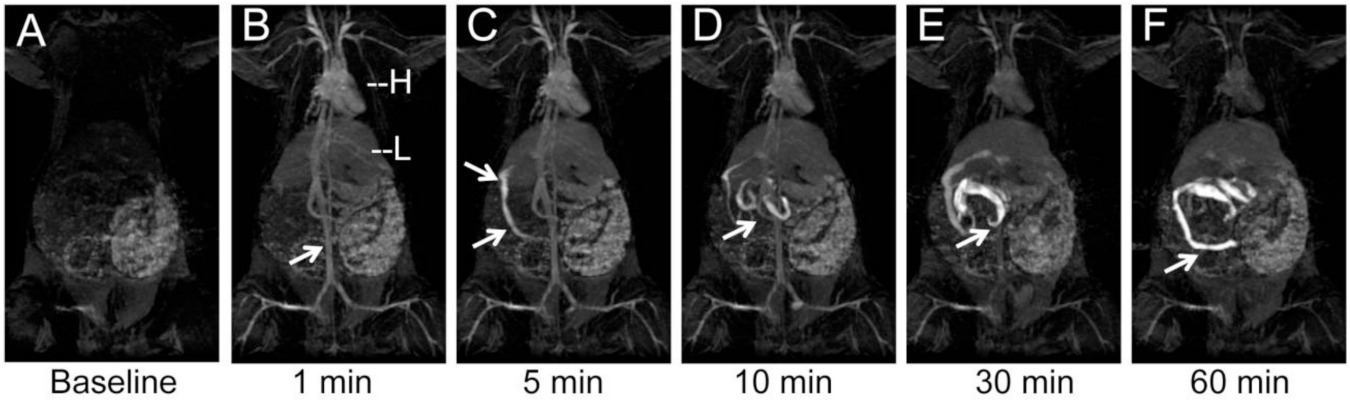

Figure 1.

3D TOF MR cholangiogram in a rat following intravenous injection of gadolinium-functionalized PFOB NP. (**A**) Baseline image showing no evidence of vasculature or common bile duct. (**B**) 1 min post-injection, the blood pool as seen in the heart, aorta (arrow), and peripheral vasculature have strong T1-weighted positive contrast from the NP that are still constrained within the vasculature. H=heart, L=liver. (**C**) Within 5 min, the NP are rapidly excreted through the common bile duct (arrows), reflecting the rapid shunt of contrast from the liver into the small intestine. (**D**). After 10 min the small intestine contains most of the contrast, that is passed on to the large intestines at 30 min (**E**) and 60 min (**F**).

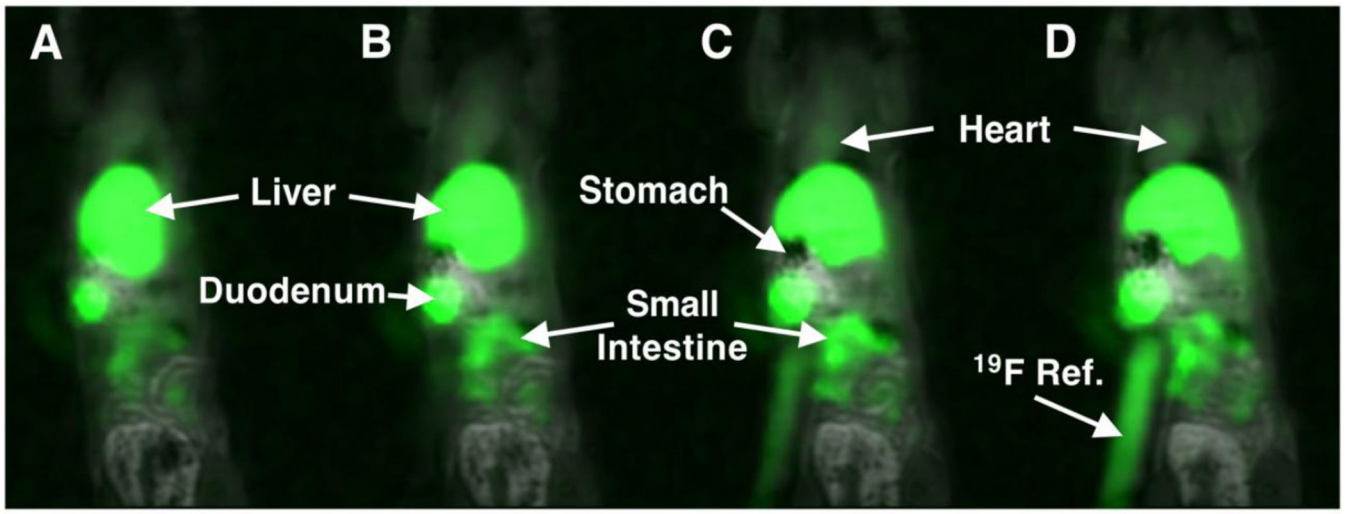

Figure 2.

(**A**–**D**). Sequential 3D overlayed $^{1}H/^{19}F$ MR images of a rat 120 min following intravenous injection of PFOB NP. NP accumulated in the liver and intestines.